AD 295 196

63-2-3

QUARTERLY STATUS REPORT
1 September to 30 November 1961

A Theoretical Study of the Modification in Echo Area of Space Vehicles Due to Their Local Space Environment

ANTENNA LABORATORY
Department of Electrical Engineering
The Ohio State University
Columbus 10, Ohio

REPORT 1116-15
Contract No. AF 19(604)-7270

1 December 1961

Astrosurveillance Sciences Laboratory
Electronics Research Directorate
Air Force Cambridge Research Laboratories
Office of Aerospace Research
United States Air Force
Bedford, Massachusetts

QUARTERLY STATUS REPORT
1 September to 30 November 1961

A Theoretical Study of the Modification in Echo Area of Space Vehicles Due to Their Local Space Environment

ANTENNA LABORATORY
Department of Electrical Engineering
The Ohio State University
Columbus 10, Ohio

REPORT 1116-15
Contract No. AF 19(604)-7270

1 December 1961

Astrosurveillance Sciences Laboratory
Electronics Research Directorate
Air Force Cambridge Research Laboratories
Office of Aerospace Research
United States Air Force
Bedford, Massachusetts

TABLE OF CONTENTS

QUARTERLY STATUS REPORT

A. PURPOSE

The change in the radar echo area of a satellite due to the plasma sheath and the density and duration of satellite induced ionization are being investigated.

B. IONOSPHERE STUDIES

1. Discoverer XXXII Observations

On October 13, 1961 the Discoverer XXXII satellite (61α γ 1) was launched in a polar orbit along with two other pieces associated with the launching. This Discoverer satellite was unique in that it was the first of this series to carry a high-frequency radio transmitter transmitting at a frequency of 20.005 Mc/s. This frequency is suitable for Faraday rotation measurements in that the Faraday nulls will occur at short intervals thus providing more increments of data in a given time. This radio frequency also allowed this laboratory to obtain Doppler information from the satellite signals on existing equipment.

A large percentage of the orbital time of this satellite was below the maximum of the F2 layer which allows an investigation of the lower ionospheric irregularities and a study of CW reflection from any induced ionization.

The radio signals of Discoverer XXXII were recorded on orthogonal dipoles in the early days of the satellite. These recorded data were retained for future analysis. The Doppler shift of the satellite's signal was frequently recorded in order to make orbital corrections to the predicted position.

2. High Frequency Studies of Satellite Induced Ionization

In monitoring the signals from standard frequency radio stations CHU, Ottawa, and WWV, Washington, it was noticed that sometimes the signal was increased in amplitude near the time of the Discoverer satellite pass. Examples of this phenomenon are shown in Figs. 1 and 2. It is possible that the signals were reflected from satellite induced ionization since the satellite itself is not large enough to support the reflection cross section needed to explain these "bursts".

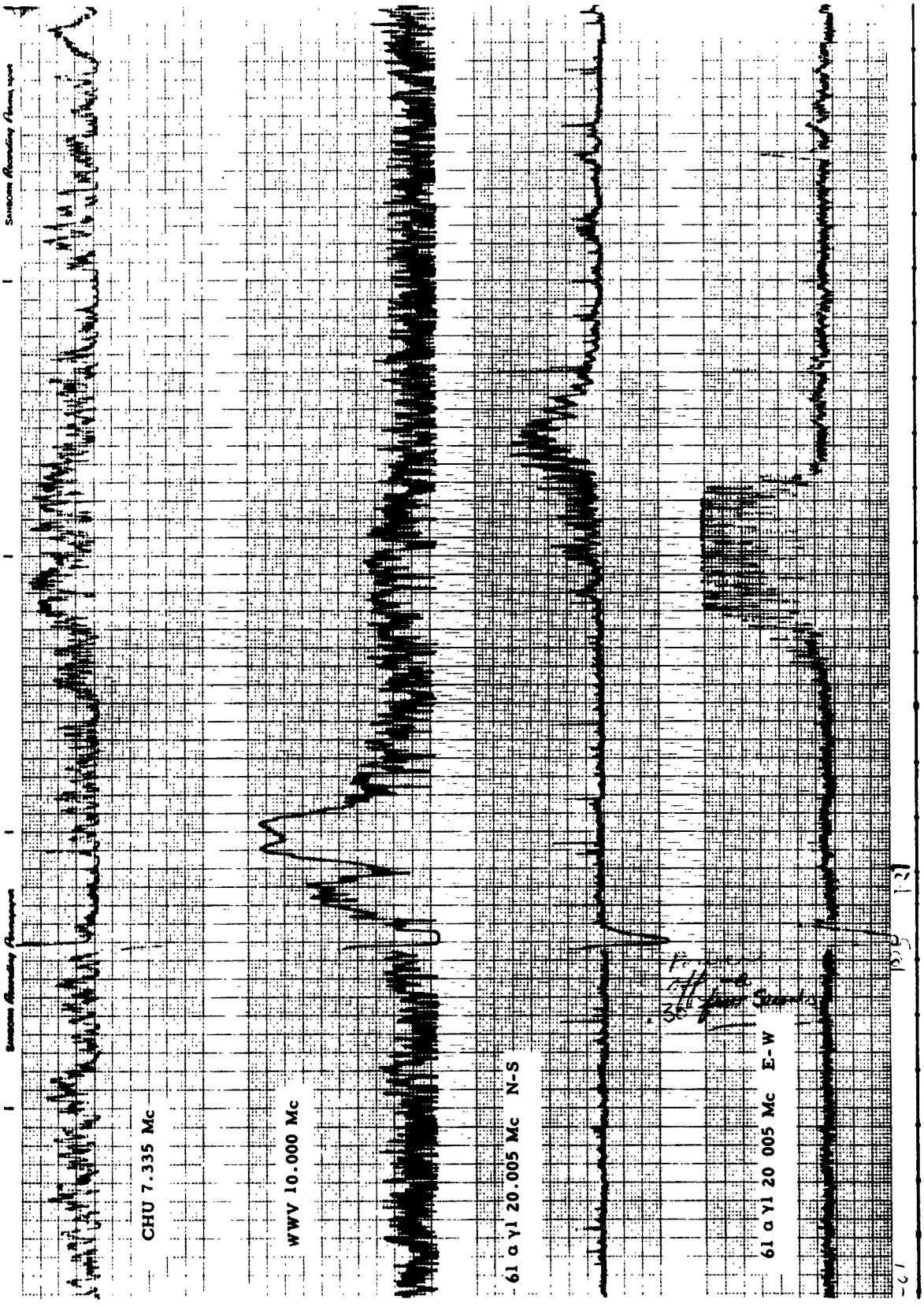

Fig. 1. WWV burst during Discoverer XXXII pass.

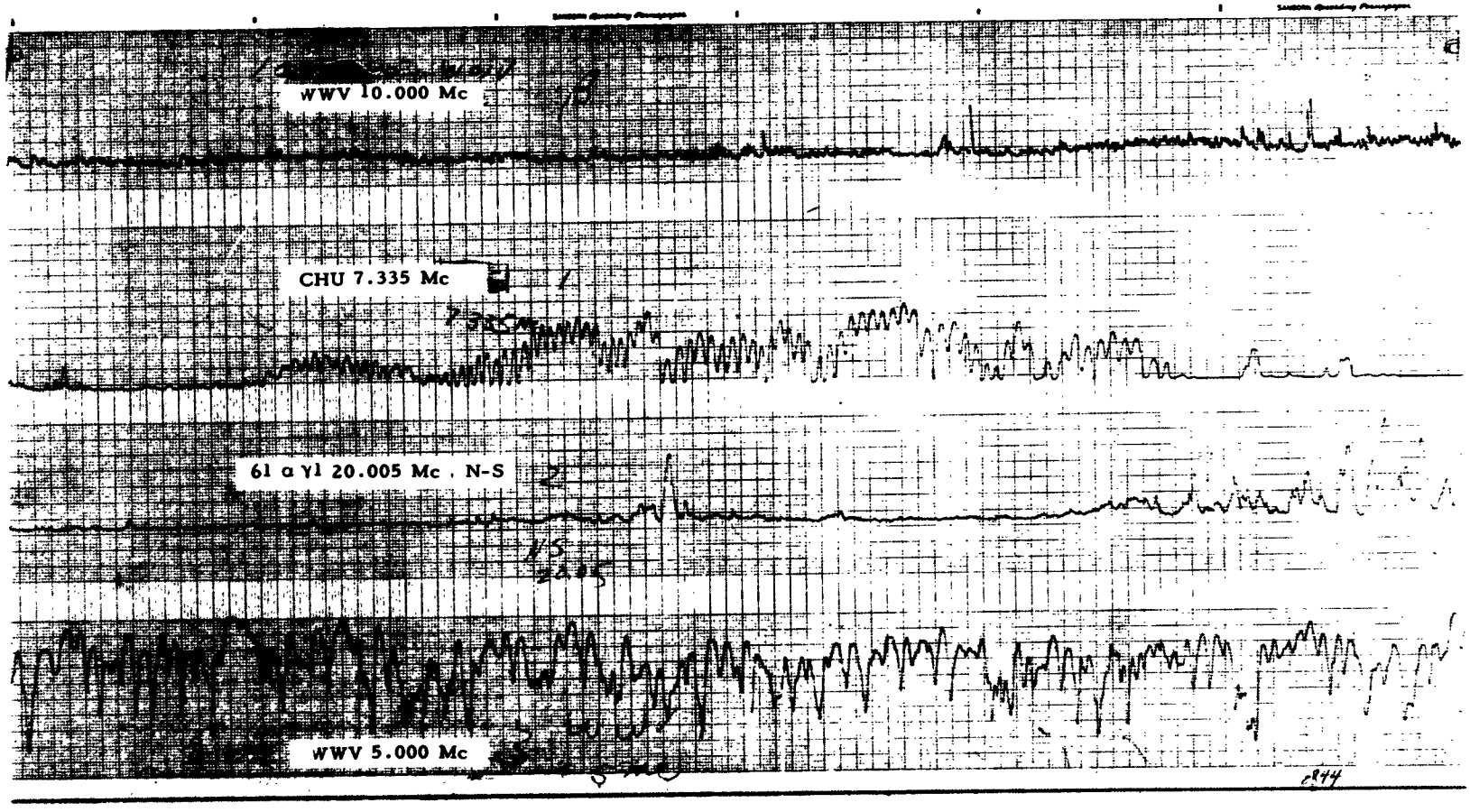

Fig. 2. CHU burst during Discoverer XXXII pass.

The Discoverer satellites appear to be perfectly suited to optimize the intensity of satellite ionization reflections because the satellites are relatively large, and the orbit has an average height in the vicinity of the F region of the ionosphere.

Considerable experimental work has been done by many investigators[1-15] in attempting to detect satellites by their influence on the ionosphere. The concensus of this work is that when a satellite is decaying (re-entering the earth's atmosphere) it may be detected consistently by enhanced CW reflections in the high-frequency band;[3] however, when the satellite is not decaying, only infrequent bursts (of CW signal) can be correlated with the passage of a satellite through the vicinity of the transmitting station and/or the observer.

It is felt that the reason for the poor correlation of the CW bursts with satellite passages is due to two reasons: (1) that may CW bursts occur naturally from ionospheric irregularities, and (2) that the correlation is usually carried out in a constrained situation which does not take into account all the parameters involved. In expanding on this second point, it is noted that in statistical and experimental techniques for correlating CW bursts with satellite passages the frequency is usually held constant, little allowance is made for the varying height of the satellite, and the variations of ionospheric conditions are usually ignored.

If one studies some proposed theoretical models of the ionization distributions about satellites such as that by Dolph and Weil,[16] it will be noted that the electron density is only perturbed by a factor of two or three. Since the electron density decays with height above the F2 layer maximum and since it will fall off by a factor of two or three within 500 kilometers[17] above the maximum, any satellite ionization above this point cannot be detected by means of reflections at the plasma frequency contour under the order of perturbations assumed, and indeed detection becomes more improbable as the height of the satellite becomes greater than that of the F layer maximum. Previous work[17] expands on this discussion, but the point is that the satellite induced ionization is most apt to yield large reflected signals when the satellite is at, or just below, the height of the F2 layer maximum.

3. Analysis of Satellite Ionization Transmission Paths

In view of the ambiguities arising in present experimental work, a theoretical study relevant to study of satellite induced ionization through high frequency reflection is being initiated. One of the preliminary results of this study is a presentation of the screening effect

of the ionosphere. In particular, WWV reflections, in which the transmitter is near Washington, D.C. and the receivers are in Columbus, Ohio, are only possible from induced ionization above the F2 layer maximum if the transmitter frequency is high enough to penetrate the ionosphere without being essentially "reflected" back to earth. Thus, to penetrate the ionosphere the transmitted frequency, f, must satisfy

$$f > f_c \sec \zeta$$

where

f_c is the critical frequency of the ionosphere, and

ζ is the angle of incidence as shown in Fig. 3.

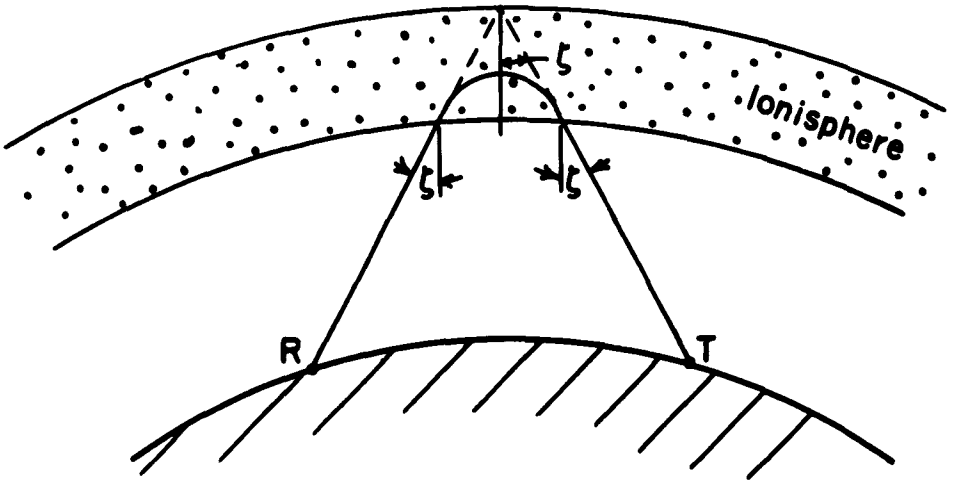

Fig. 3. Geometry of an ionospheric transmission path.

For a spherical earth[18]

$$\zeta = \tan^{-1}\left[\frac{\sin \psi/2}{1 + h/R - \cos \psi/2}\right]$$

where

R is the radius of the earth,

ψ is the angle at the center of the earth subtended by the earth radii through the two points of interest, and

h is critical height of reflection in the ionosphere.

If f and f_c are fixed, Fig. 4 shows approximately how penetration of the ionosphere can occur from the standpoint of the transmitter location and how reflected signals at frequency f can repenetrate to the observing station.

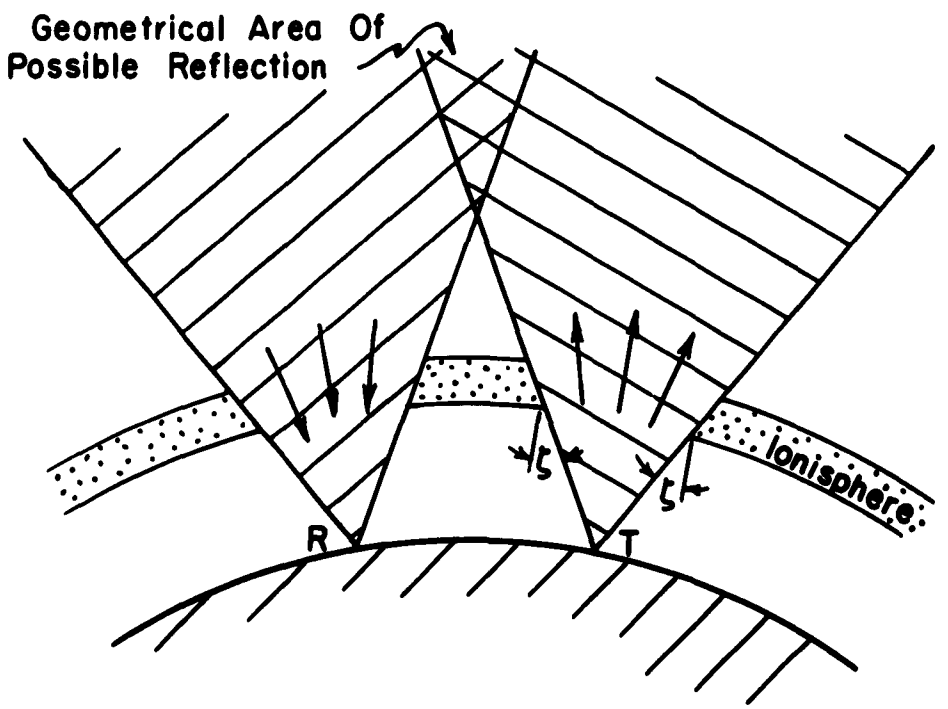

Fig. 4. Screening effect of the ionosphere relative to satellites above the F_2 layer maximum.

These areas of penetration are called "ionospheric holes"; their overlap allows the drawing of contours which enclose the maximum geometrical area of possible direct reflection from a satellite, at a fixed ratio of f to f_c, and at a fixed satellite height (assumed to be above the F layer maximum). These contours are shown in Figs. 5, 6, and 7, for three different satellite heights over Washington, D.C. and Columbus, Ohio.

At each height in these figures, there is a critical ratio $f/f_c|_{min}$ which is the lowest ratio for which any reflection area is possible. Also, at each height there is the ratio $f/f_c|_{max}$ which is the ratio required to cover all possible aspects above the optical horizon. It is emphasized that Figs. 4, 5, 6, and 7 are geometrical pictures and no allowance is made for continued refraction of the rays above the F2 layer maximum. It should be noted that the two stations which are the basis for Figs. 5, 6, and 7 are close together ($\approx$300 miles); however, when the transmitting station and the receiving station are separated by a larger distance $f/f_c|_{min}$ becomes larger and at a particular ratio the area of possible reflection is smaller. Also, in Figs. 5, 6, and 7, it is seen that the higher the frequency, relative to the critical frequency, the larger the area of expected reflection; however, the higher the frequency the less total reflection we expect from satellite induced ionization as previously discussed.

In conclusion, the analysis of CW reflection from satellite induced ionization can be divided initially into two different categories: (1) satellite is above the F layer maximum, and (2) satellite is below the F layer maximum. In the first case if the induced ionization is assumed to move with the satellite, then any CW burst will last only while the satellite is in the "area of possible reflection", (see Figs, 4, 5, 6, and 7). If the satellite is assumed to leave a trail of ionization, then CW reflection can be expected any time after the satellite enters the "area of possible reflection". The satellite will be in "radio sight" longer if the frequency and height of the satellite are higher, but both increases tend to reduce the expected magnitude of the reflection from any induced ionization. Thus, in correlating "CW bursts", the first criterion should be that the satellite is within the "area of possible reflection" for the satellite height, transmitted frequency, and the condition of the ionosphere at the time.

The analysis of CW reflections from satellites below the F layer maximum, is a subject of present interest, and the analysis will be reported in the future.

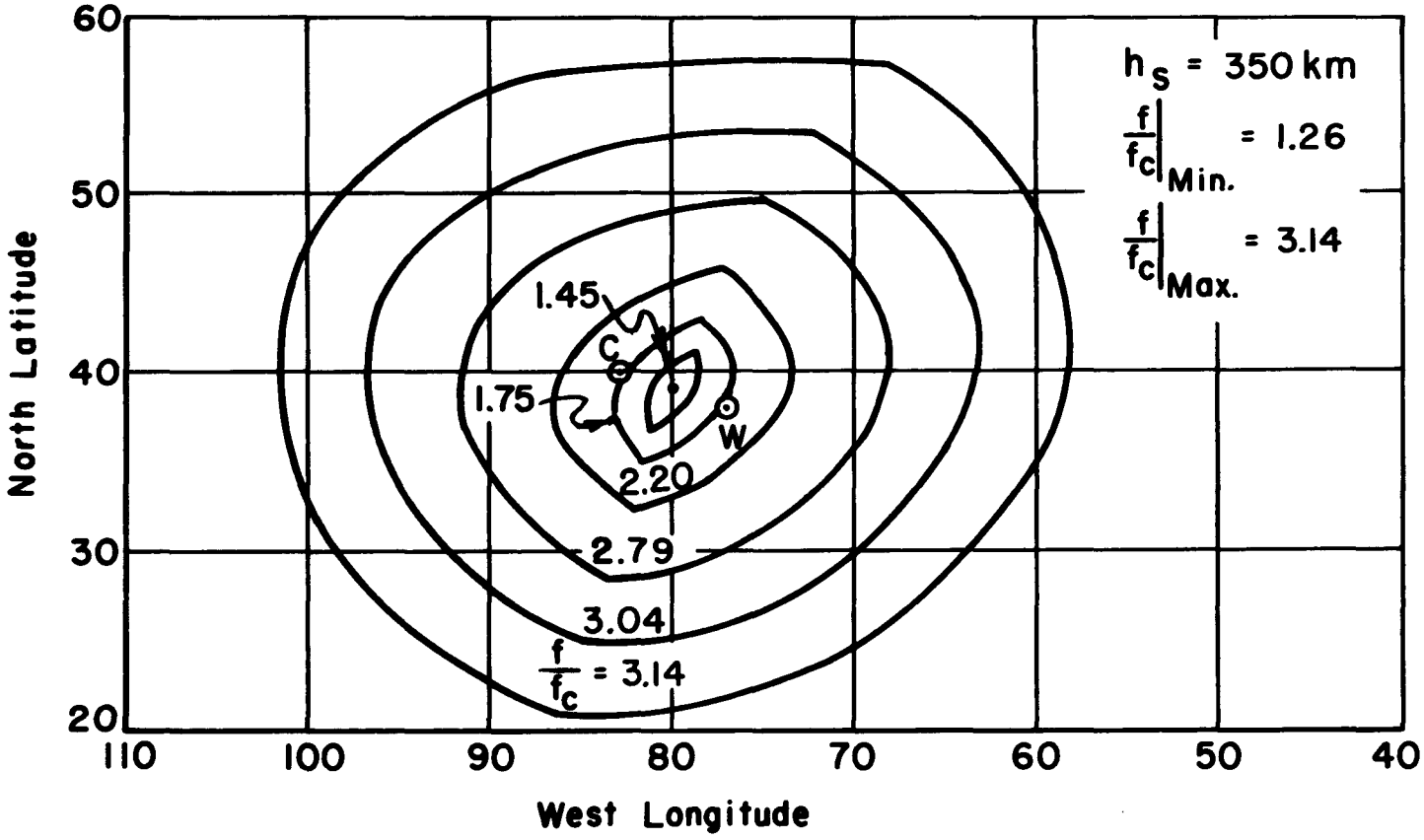

Fig. 5. Geometrical areas of possible reflection at a satellite height of 350 Km. (Assumed above F_2 max.)

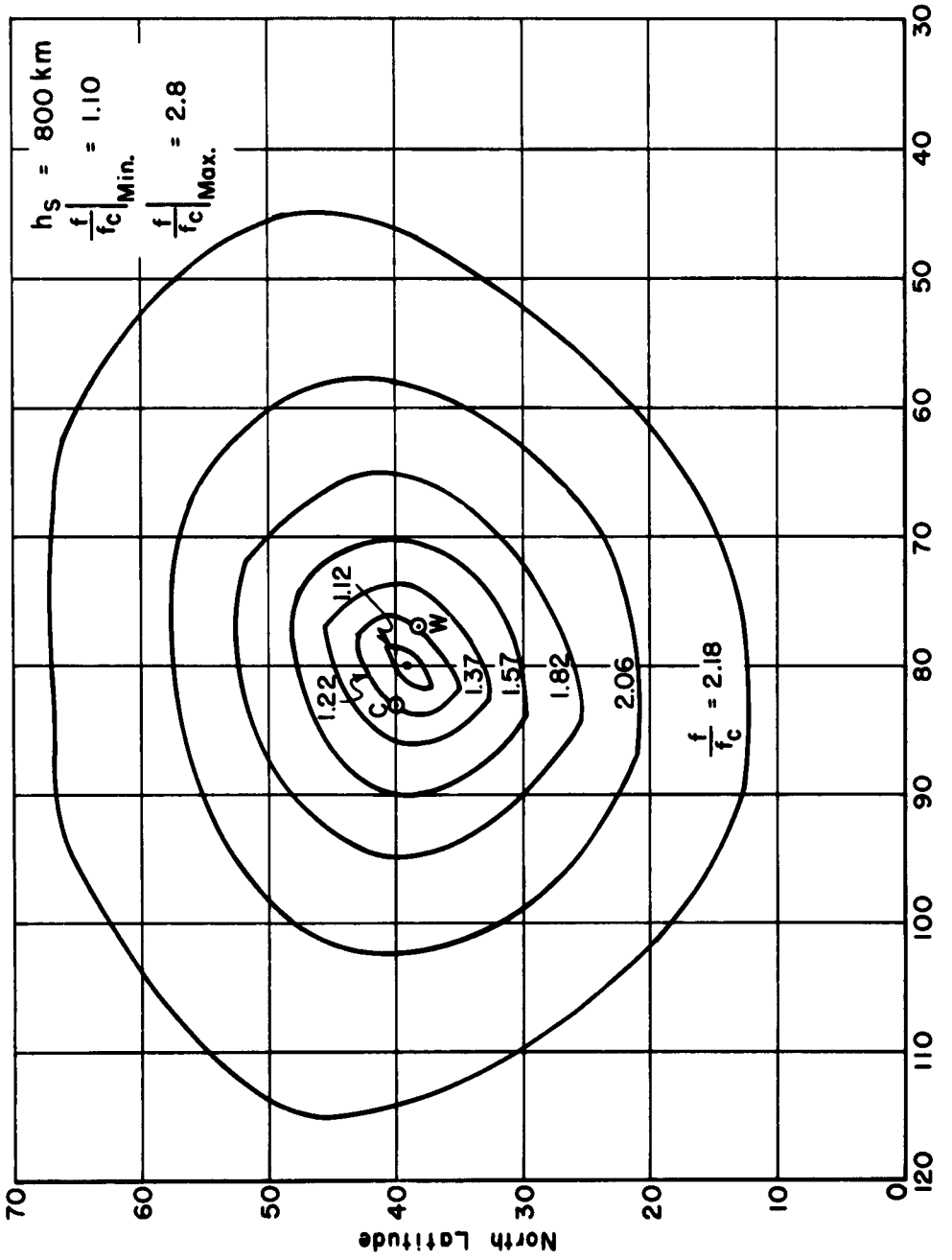

Fig. 6. Geometrical areas of possible reflection at a satellite height of 800 Km.

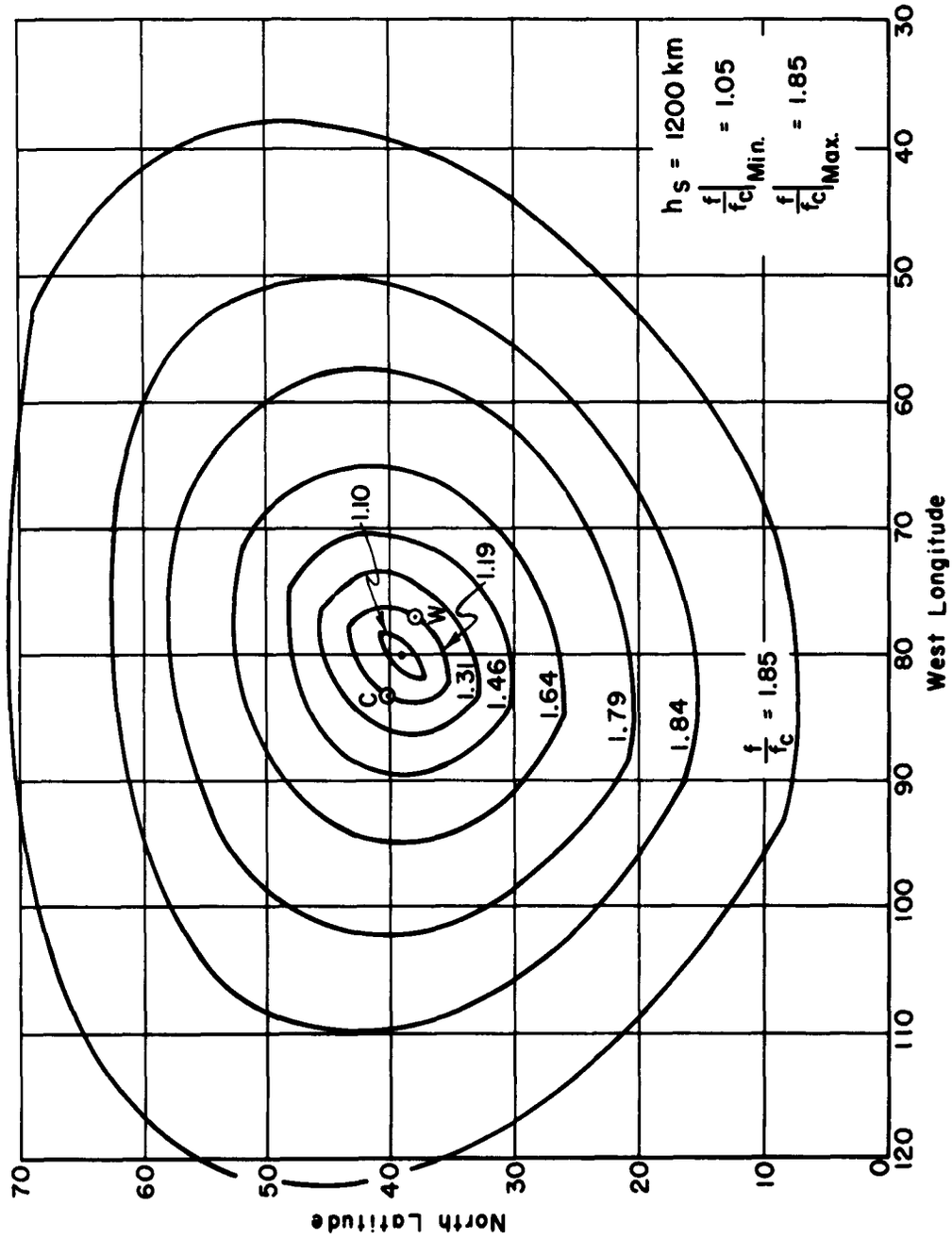

Fig. 7. Geometrical areas of possible reflection at a satellite height of 1200 Km.

C. RADAR CROSS SECTION STUDIES

1. Approximate Echo Areas of Dielectric-Coated Conducting Spheres

The superposition method (with phase correction) developed previously[19] for calculating the approximate echo area of a dielectric-clad conducting sphere has been applied to a large number of cases for a range of values, $.1 \leq \epsilon_r \leq 2$, $.02\lambda_2 \leq r_1 \leq .275\lambda_2$, and $r_1 \leq r_2 \leq 2.0\lambda_2$; where ϵ_r is the relative dielectric constant of the shell, r_1 is the inner sphere radius, r_2 is the shell radius, and λ_2 is the free space wavelength. The approximate echo areas thus calculated were compared with the exact echo areas obtained by means of an IBM 704 computer program.[19] In general, good agreement was obtained as shown by the examples of Figs. 8 and 9.

However, in several cases such as that of Fig. 10 when the dielectric shell was relatively thin, the approximate technique failed to predict an initial null or minima which occurred in the exact solution. This shortcoming may be qualitatively accounted for in the following manner: The two components considered in the superposition method, i.e., the energy reflected by the air-dielectric interface (which is assumed to be the same as that reflected by a homogeneous sphere of the same size and dielectric constant) and the energy reflected by the metallic sphere (assumed to have a modified radius $r_3 = r_1\sqrt{\epsilon_r}$ because of the focussing of rays by the dielectric shell) are essentially correct provided that the shell is sufficiently thick. For thin shells however, these components must be modified.

The focussing of rays by the air-dielectric interface which modifies the apparent radius of the inner conducting sphere may not be fully effective when the dielectric shell is thin in terms of wavelength. Comparing the field scattered by the inner conducting sphere to that which would be required to give the exact solution indicates that as the shell thickness approaches zero, the focussing effect becomes negligible and the conducting sphere appears to have its actual radius, i.e., $r_3 = r_1$. As the shell thickness is increased the effective radius of the inner sphere approaches the limiting value $r_3 = r_1\sqrt{\epsilon_r}$ at approximately an exponential rate. This suggests an equation for the effective radius of the conducting sphere having the form:

$$(1) \qquad r_3 = r_1\left[\sqrt{\epsilon_r}\,(1 - \sqrt{\epsilon_r})\; e^{-c_1\left(\frac{r_2 - r_1}{\lambda_2}\right)}\right]$$

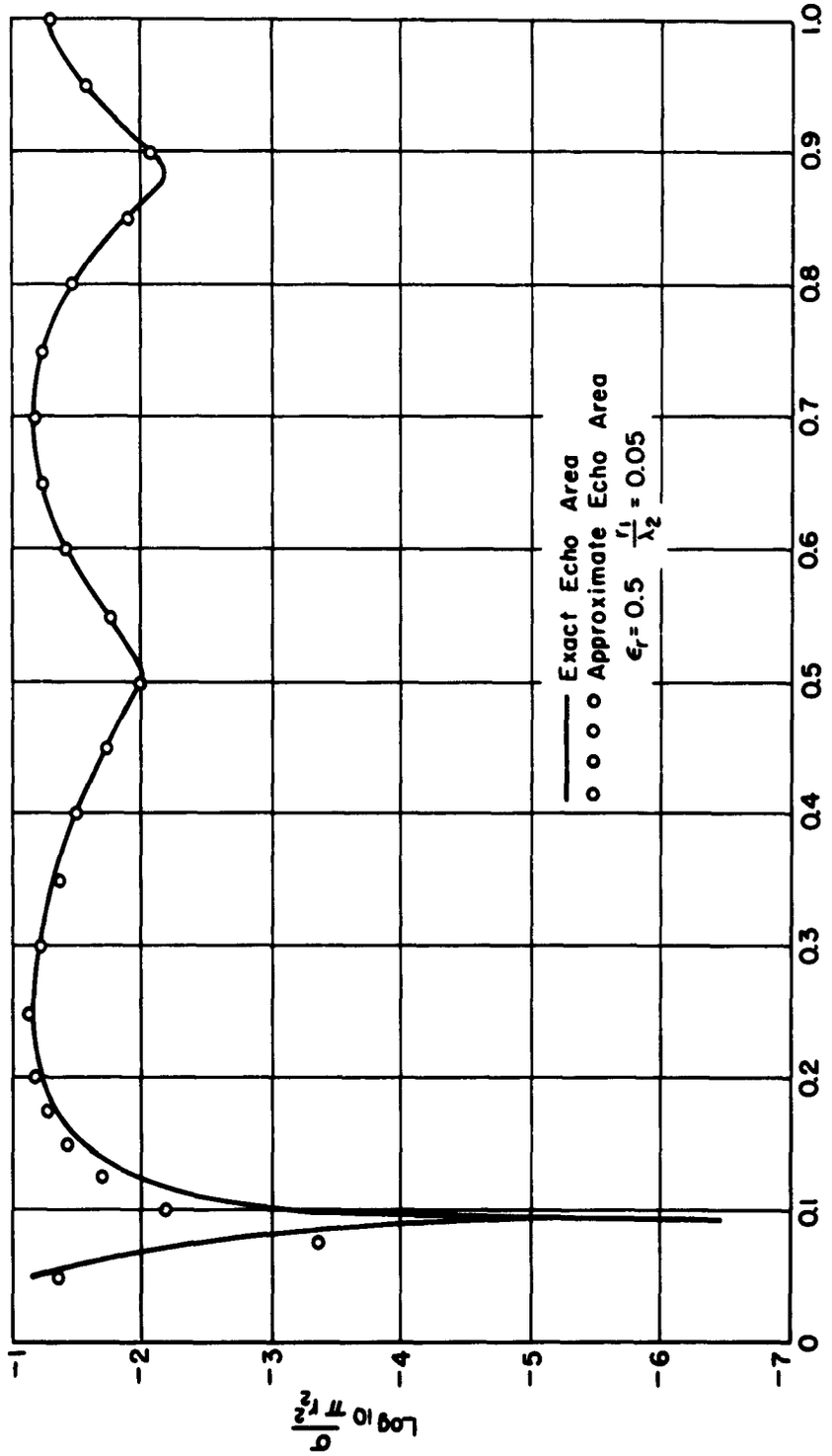

Fig. 8. Exact and approximate echo areas for a conducting sphere having a concentric dielectric shell of $\epsilon_r < 1.0$.

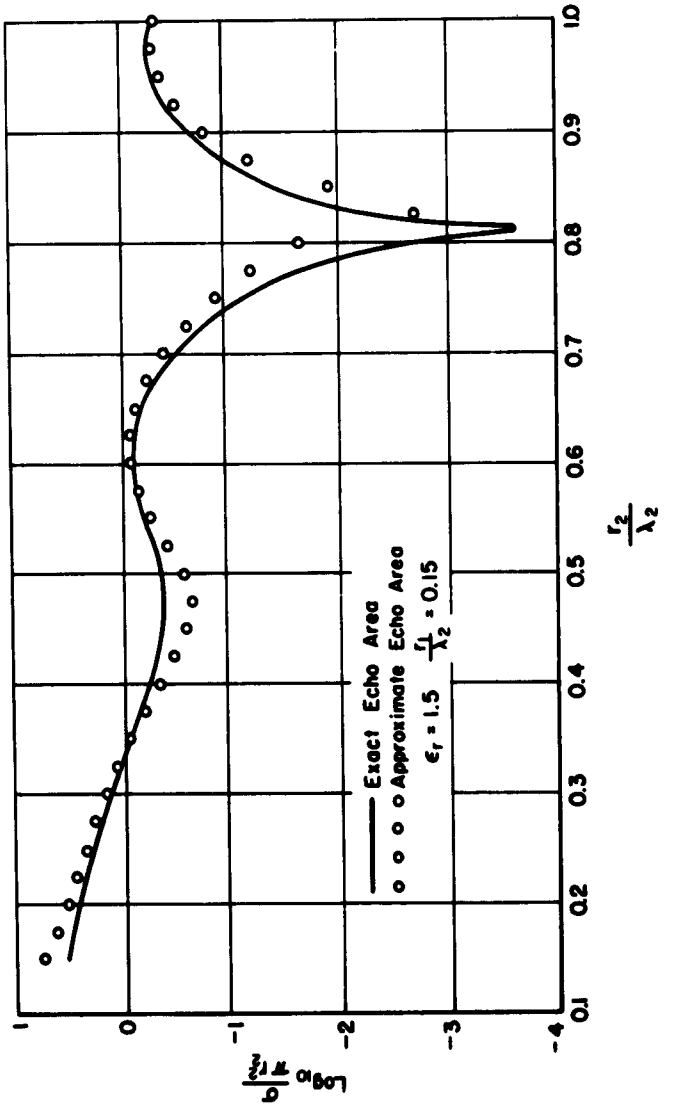

Fig. 9. Exact and approximate echo areas for a conducting sphere having a concentric dielectric shell of $\epsilon_r > 1.0$.

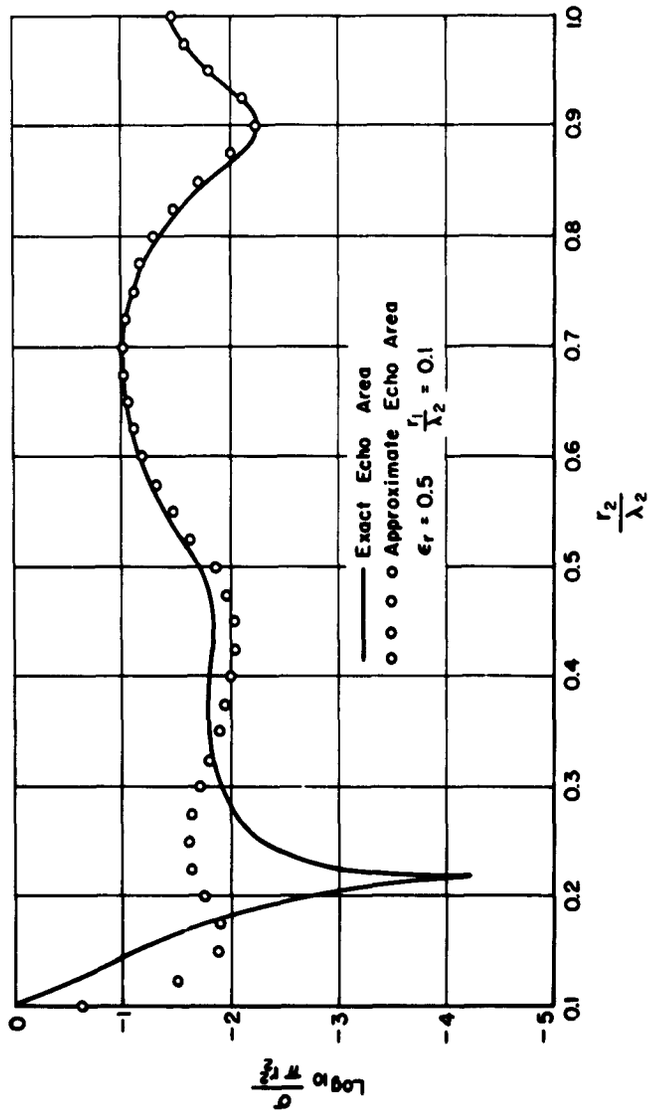

Fig. 10. Illustration of a case for which the approximate technique fails to predict an initial minima.

where

r_3 is the effective radius of the conducting sphere

r_1 is the actual radius of the conducting sphere

$\frac{r_2 - r_1}{\lambda_2}$ is the shell thickness in free space wavelengths

ϵ_r is the relative dielectric constant of the shell, and

c_1 is a constant which may depend upon r_1 and ϵ_r.

A preliminary empirical determination of c_1 from the exact solutions for several specific cases yields:

$$(2) \qquad c_1 \approx \frac{2\pi}{\sqrt{\epsilon_r}} .$$

Comparing the phase of the signal reflected by the inner conducting sphere to that required to give the exact solution for a wide range of cases yields the following general conclusions: For the shell sufficiently thick, the phase of the E-field scattered by the conducting sphere is adequately approximated by

$$(3) \qquad \phi = \phi_o + 720 \left(\sqrt{\epsilon_r} - 1\right) \frac{r_2}{\lambda_2} \text{ degrees}$$

where

ϕ = phase of E-field for the inner conducting sphere to be used in the superposition method

ϕ_o = phase of E-field scattered by a conducting sphere of equivalent radius $r_3 = r_1 \sqrt{\epsilon_r}$ in free space

ϵ_r = relative dielectric constant of the shell, and

$\frac{r_2}{\lambda_2}$ = outer radius of shell in free space wavelengths.

This is simply the phase of the signal reflected from the equivalent metal sphere adjusted to account for the change in round-trip path length through the dielectric shell as has been done previously. (Note that the path length is taken to be the entire radius of the shell, not just the shell thickness, $r_2 - r_1$; indicating that the entire sphere, not just the specular point, is an effective scatterer.)

For an infinitesimally thin shell the phase of the E-field scattered by the inner conducting sphere must approach that of the actual metal sphere in free space. Hence if the shell is relatively thin, but finite, the proper phase for the conducting sphere should lie somewhere between these limits. Empirical data indicates that a linear transition is suitable, hence to compute the phase, ϕ, in the transition region, the following equation may be used: (see Fig. 11)

$$\phi = m_1 (r_2 / \lambda_2) + b_1 \tag{4}$$

where

$$b_1 = \phi_1 - m_1 (r_1 / \lambda_2)$$

$$m_1 = \frac{y_2 - \phi_1}{x_2 - r_1 / \lambda_2}$$

$$y_2 = 720(\sqrt{\epsilon_r} - 1)\, x_2 + \phi_o, \text{ and}$$

x_2 = the value of r_2 / λ_2 at which the transition curve is assumed to end, i.e., the point at which the transition curve intersects the curve given by Eq. (3).

Examination of calculated data indicates that a suitable value for x_2 is:

$$x_2 \approx r_1 / \lambda_2 + \frac{1}{4\pi \sqrt{\epsilon_r}\; r_1 / \lambda_2} \,. \tag{5}$$

Applying Eqs. (1) and (2) to determine the amplitude, and Eqs. (4) and (5) to determine the phase (for $r_2 / \lambda_2 \leq x_2$) of the E-field scattered by the inner conducting sphere for the case of Fig. 10 yields the greatly improved approximate echo areas for five additional cases which had shown poor agreement in the thin-shell region were calculated using this thin-shell modification of the

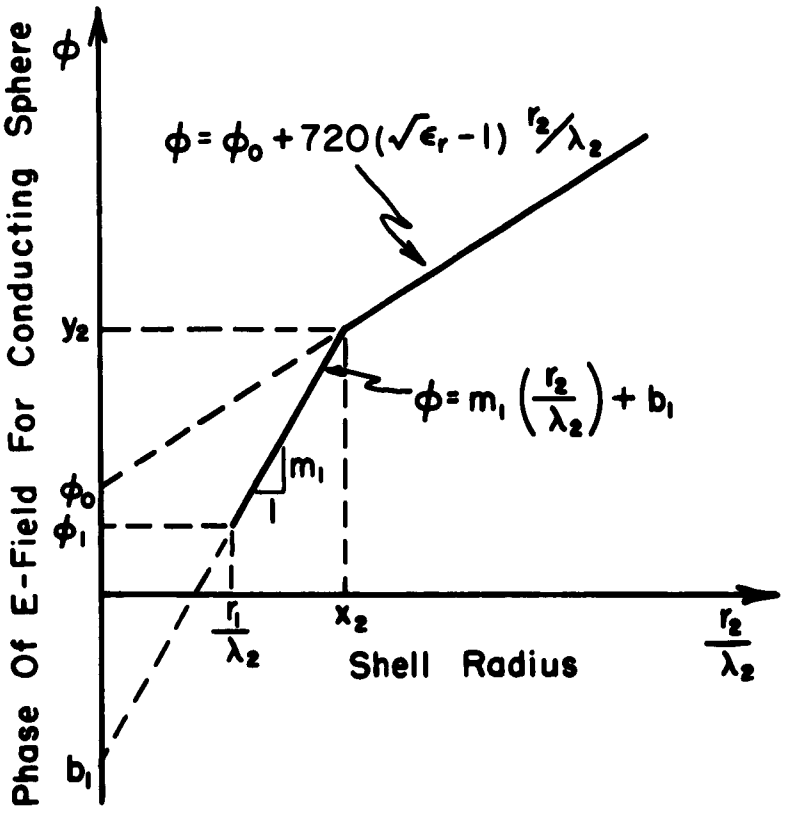

Fig. 11. Diagram for the derivation of the thin-shell linear phase curve.

superposition method. Substantial improvement was obtained in every case. A typical example of the results obtained is given in Fig. 13. Although the excellent agreement of Fig. 12 is not obtained in general, the approximate echo areas calculated by this method appear to be entirely adequate for most purposes and probably are as good as could reasonably be expected from such approximate techniques. It should perhaps be mentioned at this point that these latest refinements will not, in general, adversely effect the numerous cases which have been successfully treated by earlier versions of the superposition method. In fact, some improvement should result, although such improvement will be slight in most cases.

The major problem remaining is that of the large inner sphere (on the order of 1/2 wavelength or greater in radius). In this case it will probably be necessary to modify the E-field scattered by the dielectric shell which up to the present has been treated as a homogeneous dielectric sphere. A significant part of the rear interface will now be shielded by the conducting sphere, hence the scattering properties of the shell will be modified. As this represents a change in shape of the scatterer, rather than a change in size as was the case for modification of the inner sphere, the problem becomes more difficult. It may be necessary to employ approximate techniques[20] for determining the component of scattered field due to the shell rather than using the exact solution for the homogeneous dielectric sphere which has been used successfully when the inner sphere is small in terms of wavelengths.

2. Bistatic Echo Areas of Dielectric-Coated Conducting Spheres

The superposition method as described in the previous section has been applied to determine the bistatic echo area for a dielectric-coated spherical configuration of fixed size. The approximate echo areas computed in this manner are compared to the exact solutions in Figs. 14 and 15 which give echo areas for the E-plane and H-plane, respectively, versus bistatic angle. The agreement obtained is quite good; however, it will be necessary to investigate numerous additional cases before the general range of validity can be established. Figures 14 and 15 represent a case for which the shell is thick enough that the thin-shell amplitude equations, (1) and (2), have negligible effect; and $r_2/\lambda_2 > x_2$ so that the phase of the signal reflected by the conducting sphere is given by Eq. (3). Verification of the thin-shell modifications for bistatic scattering will require additional computer data which is temporarily not available during the replacement of the IBM 704 computer by an IBM 709 computer at The Ohio State University Numerical Computation Laboratory. The required data should be available during the next interim, however.

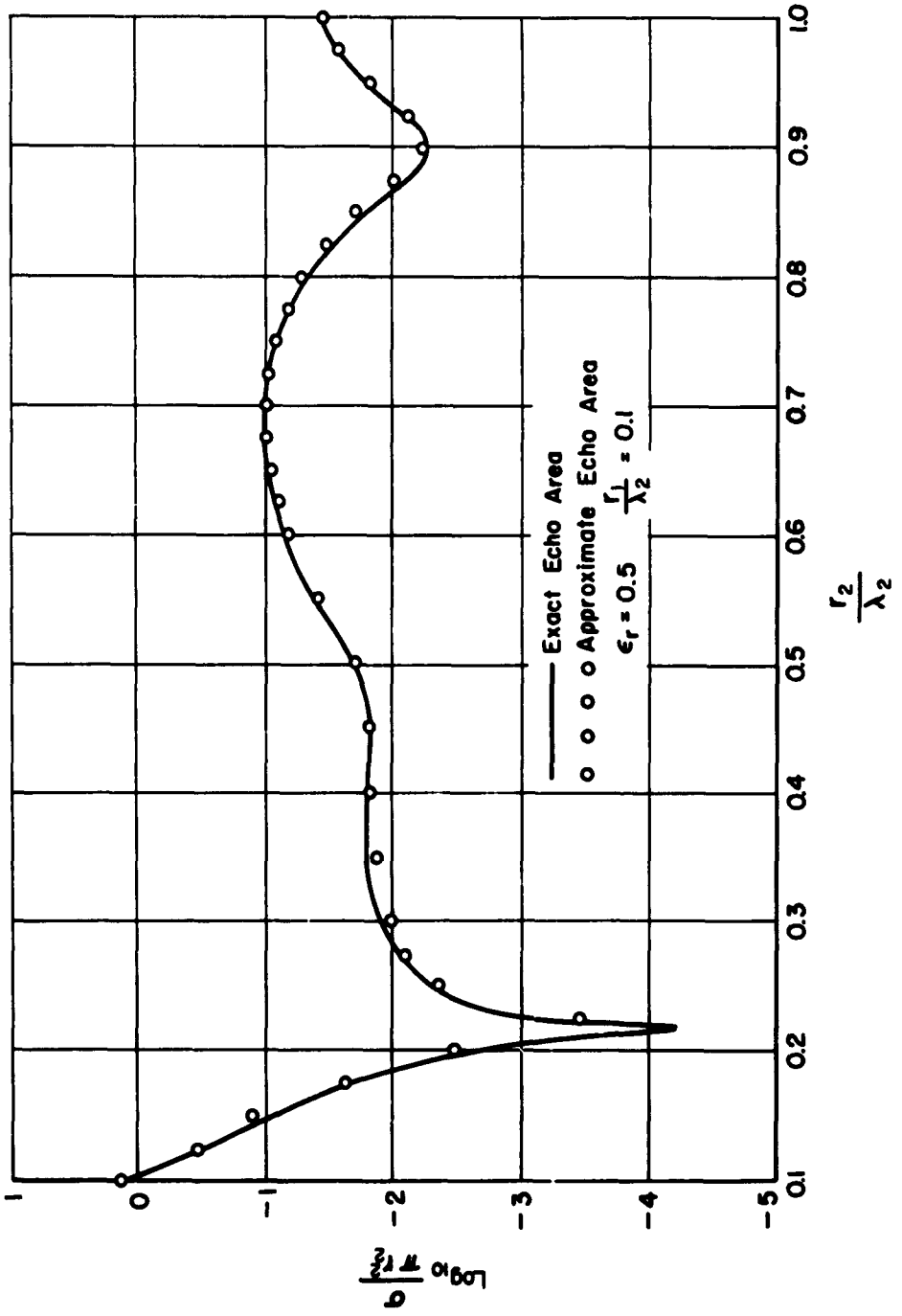

Fig. 12. The approximate echo area for the case of Fig. 10 obtained by using the thin-shell amplitude and phase corrections.

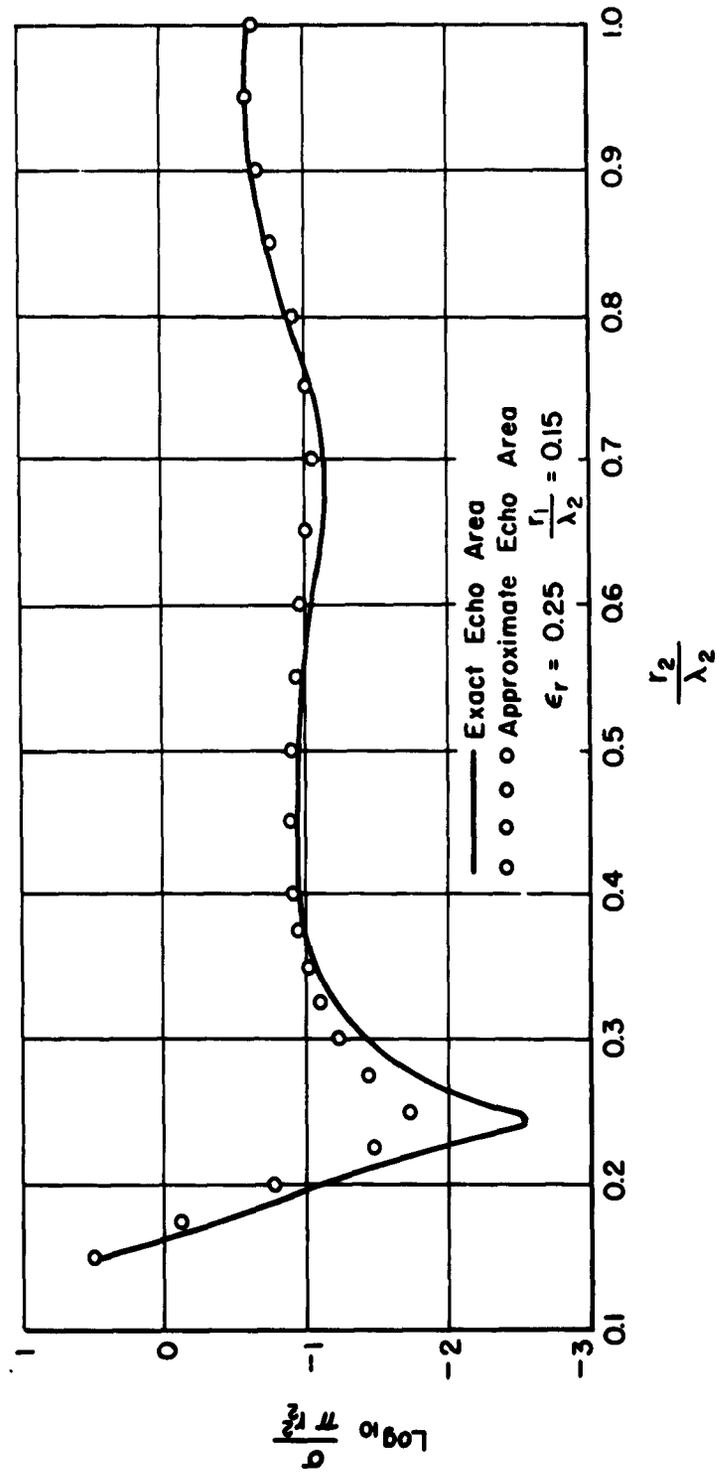

Fig. 13. A typical example of an approximate echo area obtained using the thin-shell amplitude and phase corrections to the superposition method.

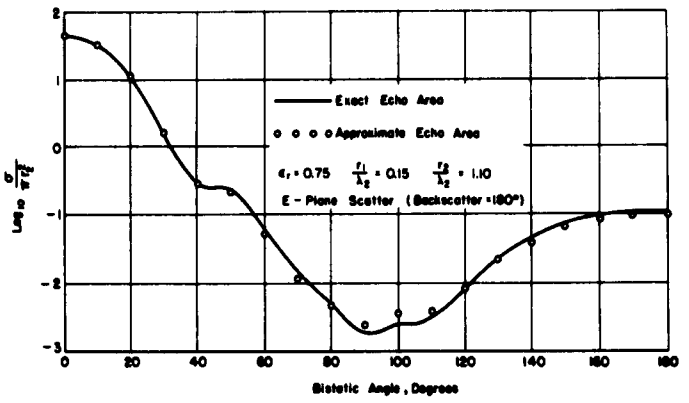

Fig. 14. Exact and approximate echo areas for E-plane bistatic scattering by a dielectric coated sphere.

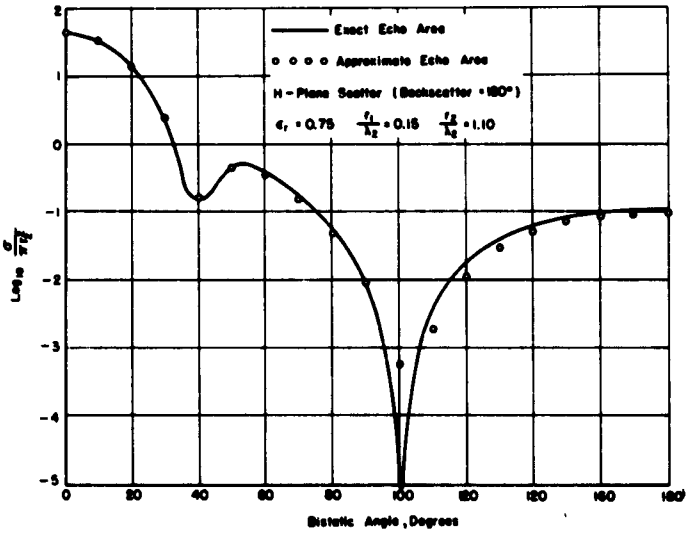

Fig. 15. Exact and approximate echo areas for H-plane bistatic scattering by a dielectric coated sphere.

3. Echo Area of a Conducting Sphere with a Non-Concentric Spherical Dielectric Shell

To date the entire effort in echo area approximation has been directed toward perfecting the case of concentric spheres, for which an exact solution is available for confirmation. The motive behind these studies is the extension of these methods to cases for which no exact solution is available. One such case is the metal sphere coated with a non-concentric spherical dielectric shell. Using the method described above requires knowledge of two characteristics of the configuration in addition to the pertinent dimensions.

First, the "apparent" size of the metal body is found from the pertinent geometry using techniques discussed in the previous interim report[19] where Snell's Laws were applied to find the apparent diameter D from the ray paths tangent to the metal sphere (see Fig. 16).

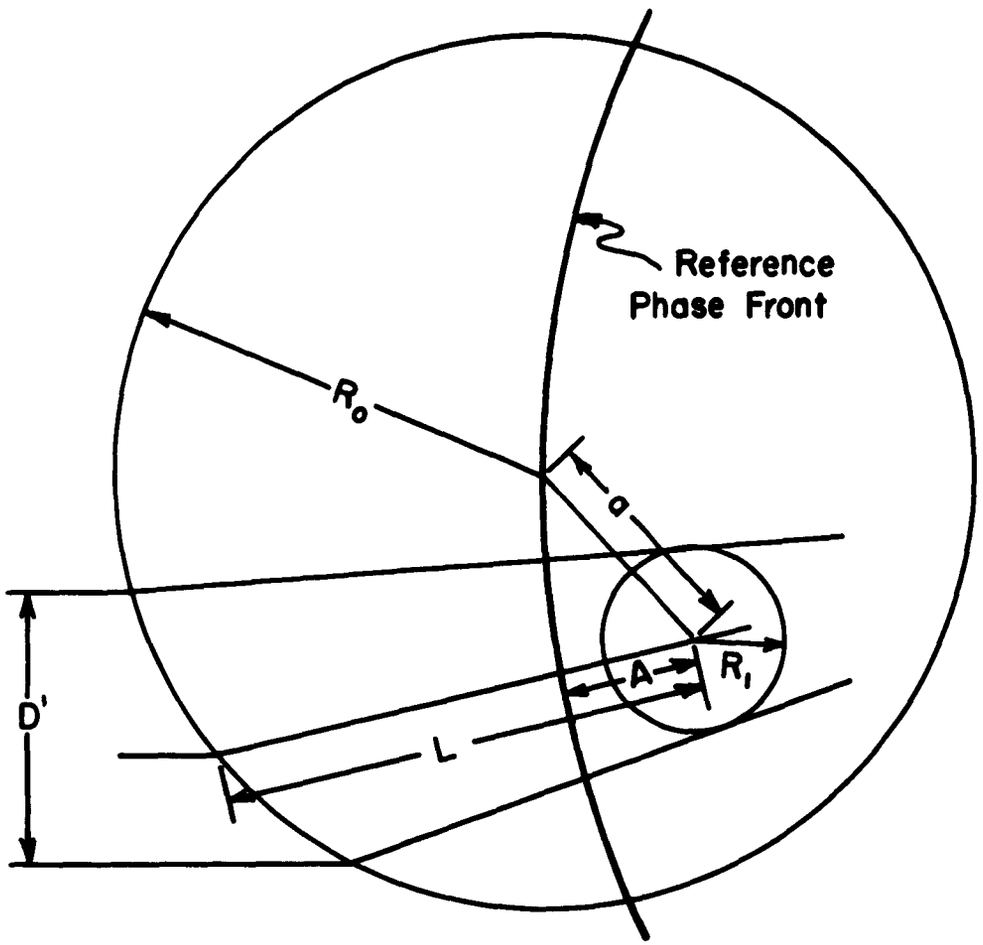

Fig. 16. Configuration of conducting sphere coated with a non-concentric spherical dielectric shell.

Second, the relative phase of the signals reflected from the metal sphere is obtained. The electrical path length in the dielectric, for thick shells, is taken to be the distance, L, of the ray to the metallic sphere center. The reference phase front of Fig. 16 is determined and the distance A computed. Since the phase of the dielectric sphere is computed relative to its center, i.e., the phase front shown, the phase of the metal sphere reflection must contain a correction proportional to A. The final phase delay of the metallic sphere reflection is

$$\phi = 720^{\circ}\left[A + (\sqrt{\epsilon_r} - 1)L\right].$$

Using these methods the echo area of such a target for which the pertinent parameters are (measured for frequency f = 9000 megacycles):

relative dielectric constant of shell $\epsilon_r = 1.80$

dielectric shell radius $R_o = 1.1811$ in. = $.9\lambda$

metal sphere radius $R_1 = .1875$ in. = $.143\lambda$

center offset of metal sphere $a = .5905$ in. = $.45\lambda$

was computed and the results are compared with experimental values in Fig. 17. The agreement is excellent, with less than 5 db deviations in the vicinity of the nulls and less than 2 db deviation elsewhere, and with identical shape throughout. Similar attempts in the following months should extend the realms of scattering knowledge significantly.

4. Reflections from a Plasma Slab at the Plasma Frequency Contour

The scattering by a thin plasma slab when the frequency f of the incident energy is in the vicinity of the plasma frequency f_p becomes important when the WWV scattering discussed in a preceeding section of this report is considered. If the plasma is infinite in extent the reflection at the interface is complete when $f = f_p$. It is not clear that this is the case when the slab has a finite thickness. In fact, at least one author[21] intimates that certain conditions must be satisfied in order that complete reflections occur at the front interface.

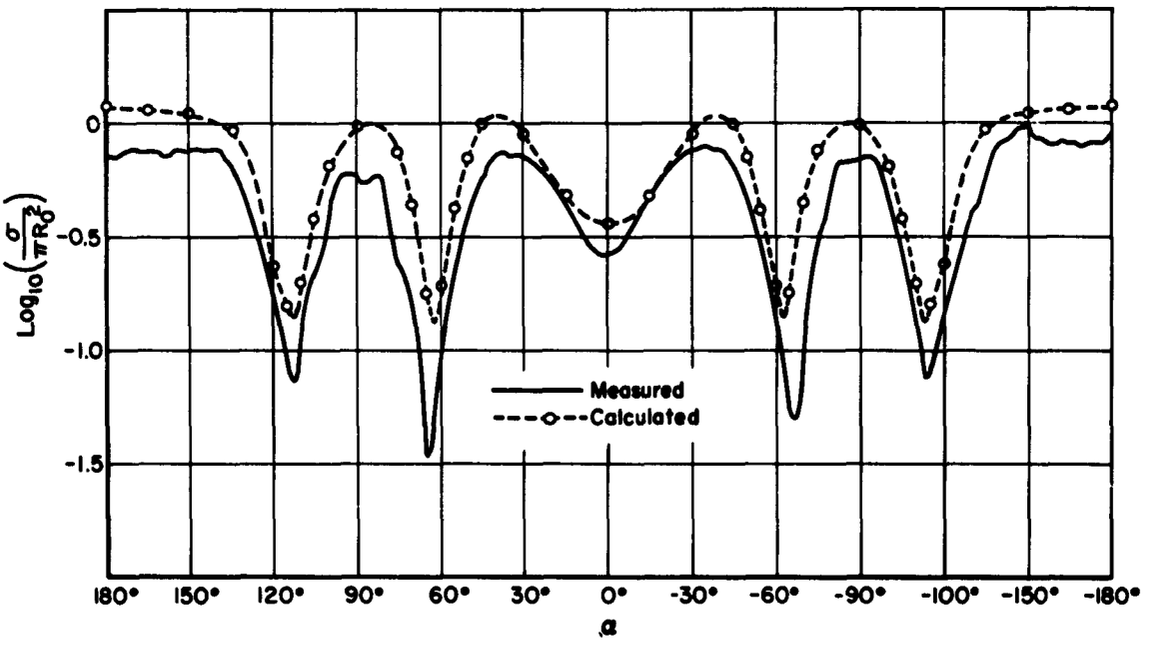

Fig. 17. Comparison of measured and calculated echo areas for nonconcentric coated sphere.

The problem may be formulated in terms of the Fresnel reflection and transmission coefficients in a simple manner if only the lossless case is considered. Essentially the same results are obtained when loss is introduced but the analysis becomes more complicated.

The reflection coefficient is given by

$$R_{12} = \frac{\sqrt{\epsilon_1} - \sqrt{\epsilon_2}}{\sqrt{\epsilon_1} + \sqrt{\epsilon_2}}$$

and the transmission coefficient by

$$T_{12} = \frac{2\sqrt{\epsilon_1}}{\sqrt{\epsilon_1} + \sqrt{\epsilon_2}}$$

where ϵ_1 = dielectric constant of the ambient medium and

ϵ_2 = dielectric constant of the plasma slab.

The ratio

$$\frac{E_R}{E_i} = R_{12} + R_{21}\, T_{12}\, T_{21}\, e^{-2j\beta x}$$

where

E_r = the reflected electric field

E_i = the incident electric field

x = thickness of the slab, and

$\beta = \omega\sqrt{\mu\epsilon}$ = propagation factor.

Substituting the appropriate values for R and T in the above ratio yields

$$\frac{E_R}{E_i} = \frac{\sqrt{\epsilon_1} - \sqrt{\epsilon_2}}{\sqrt{\epsilon_1} + \sqrt{\epsilon_2}} \left(1 - \frac{2\sqrt{\epsilon_1}\sqrt{\epsilon_2}}{(\sqrt{\epsilon_1} + \sqrt{\epsilon_2})^2}\, e^{+2j\beta x}\right) .$$

Note that when ϵ_2 vanishes the ratio goes to unity in a manner that is independent of the thickness x of the plasma slab. This result is independent of the value of ϵ_1. Therefore, in a continuously varying media such as has been suggested in various models of the ionosphere as perturbed by a satellite, complete reflection is expected at the contour where the radar frequency and the plasma frequency are equal. Similar results have been obtained when a lossy ionosphere is considered.

If the variation in dielectric constant is such that the ϵ_2 does not pass through zero, but becomes negative in a discrete step, the final term in the ratio E_r / E_i must vanish to obtain complete reflection. This will occur for a sufficiently thick sheet since the exponential $e^{j\beta x}$ goes to the form $e^{-|\beta x|}$. This is the condition[21] that has been set forth for complete reflection but in practice would not appear due to the relatively continuous nature of the ionized medium.

D. A RADAR RANGE FOR SIMULATION OF PLASMA COATED BODIES

In previous quarters research was initiated to investigate a scattering range to simulate measurement of the echo area of plasma clad bodies such that the relative dielectric constant is less than one. This was to be accomplished by means of a tank filled with a dielectric liquid having a high dielectric constant acting as the ambient medium. Then dielectric bodies with dielectric constants less than the liquid would simulate relative dielectric constants less than one. The requirements on such a liquid were determined as:

(1) relative dielectric constant $\epsilon_r > 4.0$

(2) loss tangent, tan $\delta < .01$

(3) relatively inexpensive.

Research was directed toward discovery or synthesis of a liquid having these properties. A system for measuring dielectric constant and loss tangent by the shorted-waveguide method was built and used for measuring various liquids and mixtures. Among the liquids tested were mixtures of Rutile (TiO_2) with various low-loss oils.

Of these, a mixture of 42% rutile, by volume, in transil oil was found to have the required properties. Rapid settling of the rutile from the mixture could be greatly mitigated with little change in electrical properties by replacing part of the transil oil by petrolatum to increase the viscosity of the mixture.

It has been decided not to proceed with actual construction of the scattering range. A summary report on the investigations will be forthcoming.

E. PROGRAM FOR THE NEXT INTERVAL

The Discoverer XXXVI satellite, launched December 12, 1961, has two unmodulated radio transmitters transmitting at 20.005 Mc/s and 40.01 Mc/s. The radio signals of this satellite will be recorded for the time this satellite is in orbit. The availability of these two harmonically related frequency sources in the ionosphere will make possible "dispersive polarization rotation" measurements which will allow more accurate determination of the total electron content below the satellite.

Theoretical analysis of Faraday rotation measurements is to be continued. Specified emphasis will be given to refraction and path splitting corrections. Once these corrections are obtained, it is felt that the ionospheric electron content may be studied during an entire pass of a satellite over North America.

Also, the analysis of high frequency reflections from satellite induced ionization will be continued from the point of view of developing a set of criteria which will give some insight into the probability of obtaining these reflections under various conditions. The dependence of such reflections on the height of the satellite, for example, as well as upon ionospheric conditions, are of primary interest.

Completion of approximate techniques for computing the monostatic echo area of concentric dielectric coated spheres is anticipated. In particular a major effort is to be devoted to the case of large inner spheres. Additional work is also to be devoted to the case of the concentric cylinder.

When the computer becomes operative again, additional cases of bistatic echo area of concentric spheres are to be considered. While the cases that have been treated to date have yielded good results, it is believed that discrepancies will appear and that the investigation of such discrepancies will yield additional insight into the scattering mechanisms.

Additional effort is to be devoted to the study of non-concentric spheres. It is expected that the introduction of a loss factor will further improve the excellent results already obtained. This should also point the way to applying these techniques to the studies of camouflage materials. The bistatic echo area of this configuration is also to be treated.

The study of the echo area of dielectric bodies initiated in the previous interim report is to continue. The previously reported techniques are to be extended and other methods are to be reviewed. A study of bistatic echo areas of dielectric bodies is to be incorporated in the program. It should be noted that this part of the program will be of major significance when the study of the echo area of coated bodies of arbitrary shape is begun.

BIBLIOGRAPHY

1. Kraus, J.D., "Detection of Sputnik I and II by CW Reflection," Proc. IRE, Vol. 46, 611-612, March 1958.

2. Kraus, J.D., "The Last Days of Sputnik I," Proc. IRE, Vol. 46, pp. 612-614, March 1958.

3. Kraus, J.D. and Dreese, E.E., "Sputnik I's Last Days in Orbit," Proc. IRE, Vol. 46, pp. 1580-1587, September 1958.

4. Kraus, J.D., "Evidence of Satellite-Induced Ionization Effects Between Hemispheres," Proc. IRE, Vol. 48, pp. 1913-1914, November 1960.

5. Dieminger, W., "Ground Scatter by Ionospheric Radar," AGARD Avionics Panel Meeting, Copenhagen, 20-25 October 1958, published in Avionics Research: Satellites and Problems of Long Range Detection and Tracking, Pergamon Press, New York, 1960.

6. Flambard, A. and Reyssat, M., "Ondes Electromagnetiques et Satellites Echoes des Trainees Ionisees de Satellites en H.H.," AGARD Avionics Panel Meeting, Copenhagen, 20-25 October 1958, published in Avionics Research: Satellites and Problems of Long Range Detection and Tracking, Pergamon Press, New York, 1960.

7. Hendricks, et.al., "Radio Reflections from Satellite Produced Ion Columns," Proc. IRE, Vol. 46, p. 1763, October 1958.

8. Liszka, L., "A Type of Variation of the Signal Strength from 1958δ2 (Sputnik III)," Nature, 183, p. 1384, May 16, 1959. See also "Studies of Transmissions from Satellites with Emphasis on Propagation Aspects," contribution from Kiruna Geophysical Observatory of the Royal Swedish Academy of Science, 15 October 1959, ASTIA No. AD 239 071.

9. Roberts, C.R., Kirchner, P.H., and Brag, D.W., "Radio Detection of Silent Satellites," QST, Vol. 43, pp. 34-35, August 1959.

10. Lerner, L.S., Baron, R., and Eastwood, D., "Analysis of Ballistic Missile Interception Systems, Part II: Experiments on Satellite-Correlated RF Backscatter," The University of Chicago Laboratories for Applied Science, May 1960, Contract No. AF 33(616)-5689.

11. Hame, T.G. and Stuart, W.D., "Detection of Satellites by Their Influence on the Ionosphere," paper presented at the URSI-IRE Meeting, Boulder, Colorado, December 12-14, 1960.

12. Lootens, H.T., "Satellite Induced Ionization Observed with the Doploc System," ARPA Satellite Fence Series, Report No. 23; also Report No. 1362, Ballistic Research Laboratories, Aberdeen Proving Ground, Maryland, August 1961.

13. "Final Scientific Report, Part I on Ionospheric Propagation Studies," Raytheon Manufacturing Company, Wayland, Massachusetts, 15 October 1959.

14. Croft, T.A., "An HF-Radar Search for the Effects of Earth Satellites upon the Ionosphere," Stanford Electronics Labs., Stanford University, Technical Report No. 24, March 10, 1961.

15. Soifer, R., "Satellite Supported Communication at 21 Megacycles," Proc. IRE, Vol. 49, No. 9, pp. 1455-6, September 1961.

16. Dolph, C.L. and Weil, H., "Studies in Radar Cross Sections XXXVII - Enhancement of Radar Cross Sections of Warheads and Satellites by the Plasma Sheath," Radiation Laboratory, The University of Michigan, December 1959.

17. "Quarterly Report," Report 1108-1, 16 August 1960, Antenna Laboratory, The Ohio State University Research Foundation; prepared under Contract AF 19(604)-7274, Air Research and Development Command, Laurence G. Hanscom Field, Bedford, Massachusetts.

18. "Ionospheric Radio Propagation," U.S. Department of Commerce, National Bureau of Standards, Circular 462, 25 June 1948, p. 68.

19. "Quarterly Status Report," Report 1116-13, 1 September 1961, Antenna Laboratory, The Ohio State University Research Foundation; prepared under Contract AF 19(604)-7270, Electronics Research Directorate, Air Force Cambridge Laboratories, Bedford, Mass.

20. Thomas, D., "Approximations for Backscatter from Dielectric Spheres," Report 1116-14, Antenna Laboratory, The Ohio State University Research Foundation; prepared under Contract AF 19(604)-7270, Electronics Research Directorate, Air Force Cambridge Laboratories, Bedford, Mass.

21. Eshleman, V.R., "Theory of Radio Reflections from Electron-Ion Clouds," IRE Trans., Professional Group on Antennas and Propagation, January 1955, pp. 32-39.